

Decoupling Dark Knowledge via Block-wise Logit Distillation for Feature-level Alignment

Chengting Yu^{1,2}, Fengzhao Zhang², Ruizhe Chen², Zuozhu Liu², Shurun Tan^{1,2}, Er-Ping Li^{1,2}, Aili Wang^{1,2,*},

¹ College of Information Science and Electronic Engineering, Zhejiang University

² ZJU-UIUC Institute, Zhejiang University

chengting.21@intl.zju.edu.cn, ailiwang@intl.zju.edu.cn

arXiv:2411.01547v1 [cs.LG] 3 Nov 2024

Abstract—Knowledge Distillation (KD), a learning manner with a larger teacher network guiding a smaller student network, transfers dark knowledge from the teacher to the student via logits or intermediate features, with the aim of producing a well-performed lightweight model. Notably, many subsequent feature-based KD methods outperformed the earliest logit-based KD method and iteratively generated numerous state-of-the-art distillation methods. Nevertheless, recent work has uncovered the potential of the logit-based method, bringing the simple KD form based on logits back into the limelight. Features or logits? They partially implement the KD with entirely distinct perspectives; therefore, choosing between logits and features is not straightforward. This paper provides a unified perspective of feature alignment in order to obtain a better comprehension of their fundamental distinction. Inheriting the design philosophy and insights of feature-based and logit-based methods, we introduce a block-wise logit distillation framework to apply implicit logit-based feature alignment by gradually replacing teacher’s blocks as intermediate stepping-stone models to bridge the gap between the student and the teacher. Our method obtains comparable or superior results to state-of-the-art distillation methods. This paper demonstrates the great potential of combining logit and features, and we hope it will inspire future research to revisit KD from a higher vantage point.

I. INTRODUCTION

DEEP neural networks have shown exceptional performance in several domains, including computer vision [12, 13, 19] and natural language processing [9, 35]. Nevertheless, it is common for robust and powerful networks to get advantages from large model capacity, hence resulting in significant computational and storage expenses. Various strategies have been developed to train fast and compact neural networks that are both efficient in terms of speed and size, including the invention of novel architectures [7, 17, 43, 63], network pruning [11, 25, 31], quantization [20], and knowledge distillation [16, 41, 51]. Among the investigated strategies, knowledge distillation (KD) has emerged as one of the most promising techniques to obtain a lightweight model with practicality and efficiency. KD refers to a set of methods concentrating on transferring “dark knowledge” from a large model (teacher) to a light one (student), which are applicable to a variety of network architectures and can be combined with numerous other techniques, such as network pruning and quantization [55] toward lightweight models.

The primary approaches used in KD can be categorized into two main streams: 1) logit distillation and 2) feature distillation. The earliest concept of KD was proposed based

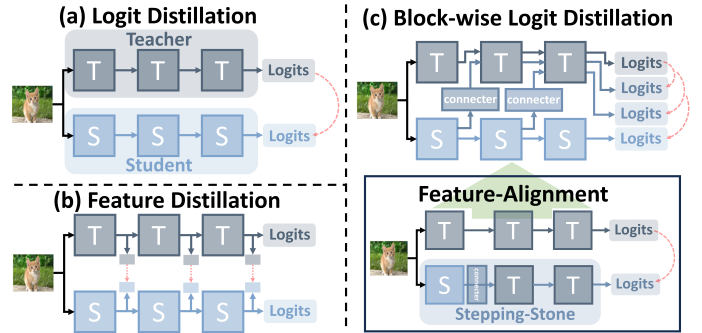


Fig. 1. Method Illustration. (a) Logit distillation transfers the entire dark knowledge based solely on output logits. (b) Feature distillation further implements feature alignment at multiple levels. (c) The proposed block-wise logit distillation framework accomplishes implicit feature alignment via output logits of stepping-stones. We refine the distillation into logit-only objectives, with the transfer of dark knowledge decoupled at the block level.

on logits [16], which transfers only logit-level knowledge from teacher to student by minimizing the KL-Divergence between prediction logits (Fig. 1a). Since then, towards better utilization of teacher knowledge [41], the majority of KD study has been dedicated to investigating intermediate layers and performing distillation via the alignment of feature distributions [5, 14], which are referred to as feature distillation (Fig. 1b). Nevertheless, recent work [65] reveals and improves the limitations of the classical KD loss and re-examines the potential of the logits, bringing the simple logit-based KD back into the limelight.

Logits or features? Although both logit-based and feature-based methods implement the distillation, they do so with quite different perspectives on the “dark knowledge”, deciding between the two very hard. It’s time to gaze at the gap between them to discover an avenue to connect the two lines together. For logit-based methods, “dark knowledge” is thought to be fully contained in the output logits, so aligning the logits is sufficient to transfer the “dark knowledge” from teacher to student (Fig. 1a); however, for features-based methods, this alignment requirement is extended to the hidden features across different block-levels in an effort to transfer different levels of “dark knowledge” by aligning block-wise features (Fig. 1b). Clearly, the features-based methods are more hypothetical and implemented with more stringent constraints in the hopes of facilitating the transfer of “dark knowledge”

to the student at finer levels; as a result, this approach may frequently converge faster and achieve a good performance. Meanwhile, in some cases, end-to-end logit-based alignment is more secure for transferring "clear" knowledge since feature-based alignment may also preserve task-irrelevant noise items throughout the distillation process. We argue that, although feature-based approaches have more success than logit-based methods at conveying "dark knowledge" through block-wise alignments, they are restricted by the need for excessively stringent alignment constraints.

Inspired by this observation, we propose a new distillation framework called block-wise logit distillation, which implements the alignment of feature-level "dark knowledge" based on the unified logit-based distillation of intermediate stepping-stone models (Fig. 1c) to fill in the gap between features and logits. As the implicit intermediate models during training, the student's shallow blocks are gradually substituted with the teacher's to establish stepping-stones, which are eventually abandoned during inference. We further evaluate the proposed methods on several visual benchmark datasets, including CIFAR100, ImageNet, and MSCOCO datasets for image classification and object detection tasks. The experimental results demonstrate that our method consistently outperforms both logit- and feature-based distillation methods. Further experiments on natural language processing tasks based on the BERT model have also been included in the experimental section to demonstrate the versatility of our approach. Additionally, a comparative analysis of training costs against related distillation methods yields several key insights: 1. Compared to feature-based KD methods, our approach not only achieves superior performance but does so with a similar degree of added complexity, highlighting the efficiency of the proposed framework without significantly increasing computational demands. 2. Regarding adaptability, we have formulated a lightweight version of the original framework that considerably diminishes the complexity typical of the standard method while still preserving high accuracy, which offers a feasible solution for contexts where computational resources are scarce. 3. The framework is compatible with recent logit-based KD approaches, providing an alternative option that can further enhance performance, which underscores the versatility of our method, rendering it an invaluable asset for augmenting the effectiveness of logit-based knowledge distillation.

II. RELATED WORK

The concept of knowledge distillation [16] was first proposed as a learning strategy that employs a larger teacher network to steer the training process of a smaller student network for various tasks [27, 28]. The working mechanism of vanilla KD is often comprehended via the process of "teaching" [51], whereby the transfer of "dark knowledge" occurs through the use of soft labels, known as logits, provided by the teacher to the student. Recent studies examine how to select, express, and transfer the "dark knowledge" more practically and effectively, which can be categorized into two main types: logit- and feature-based distillations.

Logits Distillation. In the wake of the earliest KD method based on temperature-regulated distillation [16], previous

logit-based methods have concentrated mainly on effective regularization and optimization methods. DML [64] proposes a mutual learning method to train students and teachers simultaneously. TAKD [34] proposes using intermediary "teacher assistants" to transmit knowledge in a step-by-step manner in order to narrow the performance disparity between teachers and students. Additionally, several works [6, 39] focus on interpreting the principles underlying KD. Recently, DKD [65] introduces an improved logit-based objective by decoupling the classical KD loss, which re-explores the potential of logit-based methods with comparable performance gains.

Feature Distillation. To further enhance knowledge distillation, feature distillation is proposed to perform alignments on intermediate features as well as logit outputs, which can directly transfer teacher representations [5, 14, 15, 41] or the correlation [36, 37, 47, 48] from the teacher to the student. Feature methods are more likely to obtain high performance with extensive information from the teacher; however, tight feature alignment frequently relies on prior empirical observation and meticulous adjustment of hyperparameters.

III. METHODOLOGY: BLOCK-WISE LOGIT DISTILLATION

A. Background and Notations

Given an input image X with targets Y , we let $Y^S = S(X)$ and $Y^T = T(X)$ represent the output logits of the student S and the teacher T , with

$$S = \{S_1, S_2, \dots, S_n, S_c\}, T = \{T_1, T_2, \dots, T_n, T_c\} \quad (1)$$

where n denotes the number of blocks, S_i and T_i represent i -th block separated by downsampling layers, S_c and T_c represent the fully connected layers that are employed for the final classification. Then, the process of generating intermediate features $F^S = \{F_i^S\}_{i \leq n}$ can be denoted as:

$$F_i^S = S_i \circ \dots \circ S_1(X) \quad (2)$$

We refer to \circ as nesting of functions where $g \circ f(x) = g(f(x))$. Given the task objective based on student output Y^S and the ground-truth targets Y , we define the cross-entropy loss for the classification task:

$$L_{task} = CE(\text{softmax}(Y^S), Y) \quad (3)$$

In knowledge distillation, an extra objective $L_{distill}$ is determined to measure the distance between S and T . As for logit distillation, one tries to match the softened outputs logits of student and teacher via a given distance measurement, denoted as d^L , usually applied by a KL divergence loss:

$$\begin{aligned} L_{distill} &= L_{logit} = d^L(Y^S, Y^T) \\ &= \tau^2 KL(\text{softmax}(\frac{Y^S}{\tau}), \text{softmax}(\frac{Y^T}{\tau})) \end{aligned} \quad (4)$$

Hyperparameter τ , referred to as temperature, is introduced to put additional control on softening of the signal arising from the output of the teacher network. On the other hand, feature distillation utilizes the objective to measure the distance between intermediate features, denoted as d^F , as the distillation loss of the student features and teacher features:

$$L_{distill} = L_{feature} = d^F(F^S, F^T) \quad (5)$$

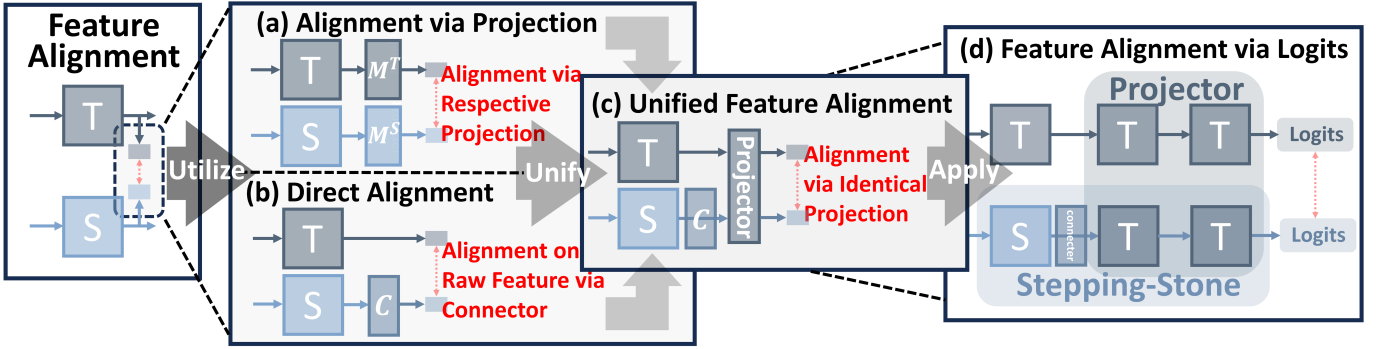


Fig. 2. Implementations of Feature Alignment. (a-b) Methods typically employed in feature distillation. (c) The proposed consolidation of alignments with identical projections. (d) Implicit feature alignment utilizing logit distillation with stepping stones. The further extension of implicit logit-based feature alignment is in Fig. 3.

The student is then trained under the integrated objectives:

$$L = \alpha L_{task} + \beta L_{distill} \quad (6)$$

where α and β are second hyperparameters controlling the trade-off between the two losses.

B. Feature Alignment: The Missing Piece of Logit-based Distillation

The primary distinction between the two types of distillation lies in the measurement of the distance between T and S . Feature-based methods tend to extract more detailed information from the feature maps, whereas logit-based methods primarily concentrate on the final output. The fundamental principle of feature distillation is to achieve feature alignment by defining and reducing the feature distance $L_{feature} = d^F(F^S, F^T)$. Due to the distinct shapes of T and S 's intermediate features, it is necessary to convert the features of both entities to a uniform size prior to continuing the alignment procedure.

There are essentially two categories of alignment methods. As depicted in Fig. 2a, one strategy is to entrust transformation modules, denoted as module M^T and M^S for T and S , which facilitates the mapping from the feature space to the latent space. The distance between features can then be determined using the projection of two features:

$$d^F(F^S, F^T) = \sum d_i^F(M_i^S(F_i^S), M_i^T(F_i^T)) \quad (7)$$

where M_i^S and M_i^T are the projection transformations for F_i^S and F_i^T , employed in various studies including attention maps [60] and factors [23]. Despite the decrease in dimensionality, previous studies have reported that the extracted feature representation does indeed result in enhanced performance. However, this highly constructive method may frequently require good priors and careful adjustments. The observation has been made that the process of projecting from a high-dimensional space to a low-dimensional space inherently results in a substantial loss of information [14]. Several approaches [5, 14] have been proposed to enhance transformations by utilizing a more robust prior, as depicted in Fig. 2b, which explicitly

defines the mapping function from the student space F^S to the teacher space F^T :

$$d^F(F^S, F^T) = \sum d_i^F(C_i(F_i^S), F_i^T) \quad (8)$$

where C_i is the connector utilized to acquire identical shapes of teacher features. Under the current setting, the process of feature alignment demonstrates a remarkable capacity for mitigating information loss; in addition, this method does not require the use of a meticulously crafted prior for feature extraction. It is crucial to recognize, however, that this method may result in a rigid alignment with task-irrelevant noise in the feature alignment.

C. Implementing Feature Alignment via Logits

Drawing inspiration from the existing feature alignment methods, we note that distinct implementations can be further refined into a unified and straightforward form for feature alignment (Fig. 2c), which is defined as:

$$d^F(F^S, F^T) = \sum d_i^F(M_i^P(C_i(F_i^S)), M_i^P(F_i^T)) \quad (9)$$

where C_i is a connector to align the number of channels between the student feature map F_i^S and the teacher feature map F_i^T . M_i^P is a shared mapping from high-dimension to low-dimension for both T and S . Currently, the process of feature alignment is executed within the projected space. It is important to highlight that our design aims to achieve the desired outcome of filtering the high-level features, extracting task-related information that is relatively clean, and conducting feature alignment via the "dark knowledge" inside the latent space. A clearer picture emerges once well-trained teacher blocks are utilized as common projectors:

$$M_i^P = T_c \circ T_n \circ \dots \circ T_{i+1} \quad (10)$$

At that time, since

$$M_i^P(F_i^T) = T_c \circ T_n \circ \dots \circ T_{i+1}(F_i^T) = Y^T \quad (11)$$

The objective of feature alignment, $L_{feature}$ in Eq. 9, becomes:

$$d^F(F^S, F^T) = \sum d_i^F(M_i^P(C_i(F_i^S)), Y^T) \quad (12)$$

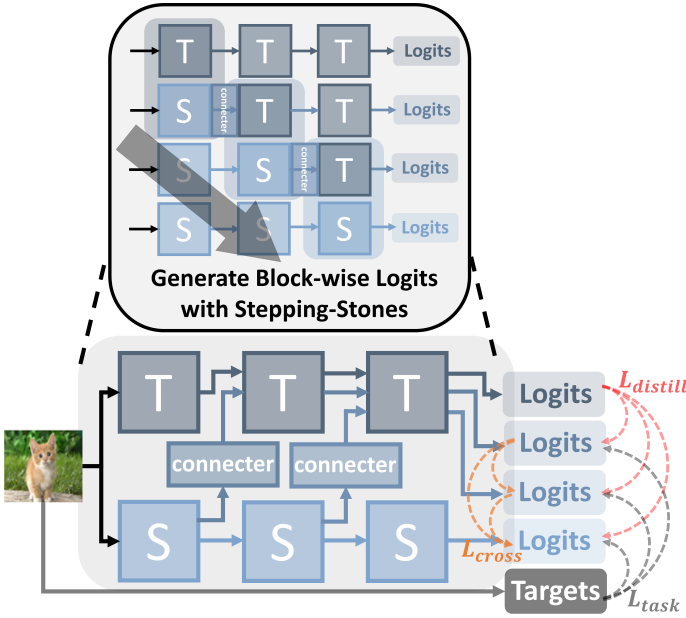


Fig. 3. Framework Overview of Block-KD. The stepping stones are executed implicitly within the fundamental dataflow to generate step-by-step logits. The final objectives are defined merely in terms of output logits.

Hence, by employing the proposed alignment method, it becomes feasible to execute feature alignment on the teacher’s logits without the need for a dedicated definition projector (Fig. 2d). Additionally, leveraging the trained deep blocks from the teacher allows for mitigating the impact of noisy items on the feature alignment to a significant extent. One of the most intriguing aspects of this particular structure is its ability to integrate feature distillation into logit distillation, as we introduce a series of intermediate models, denoted as N_i , serving as stepping stones in the overall process with output logits Y^{N_i} :

$$N_i = T_c \circ T_n \circ \dots \circ T_{i+1} \circ C_i \circ S_i \circ \dots \circ S_1 \quad (13)$$

$$Y^{N_i} = N_i(X) \quad (14)$$

where C_i follows the pre-definition that connects the intermediate output of F_i^S into the required input size of F_{i+1}^T . Now, as shown in Fig. 2d, a meticulously designed framework for achieving feature alignment has been developed:

$$\begin{aligned} d_i^F(M_i^P(C_i(F_i^S)), Y^T) &= d_i^F(N_i(X), Y^T) \\ &= d^L(Y^{N_i}, Y^T) \end{aligned} \quad (15)$$

The definition leads us to the unified distillation format as the definition for logit distillation (Eq. 4) and feature distillation (Eq. 5), which apply stepping-stone models to generate intermediate logits for features alignment.

D. Training Objectives of Overall Framework

With the discussed concept, we establish stepping-stones, N_i , for feature alignment:

$$N_i = \{S_1, \dots, S_i, C_i, T_{i+1}, \dots, T_n, T_c\} \quad (16)$$

The training objective for each stepping-stone, N_i , is defined to be consistent with the S form:

$$L^{N_i} = L_{task}^{N_i} + L_{distill}^{N_i} \quad (17)$$

where $L_{task}^{N_i}$ denotes the loss incurred by N_i with respect to the task objective, which is computed using cross-entropy loss in the context of classification tasks. $L_{distill}^{N_i}$ refers to the discrepancy between the output logits and the teacher logits in the logit-distillation process. Currently, the overarching aim of the training is articulated as:

$$\begin{aligned} L &= (L_{task}^S + L_{distill}^S) + \sum (L_{task}^{N_i} + L_{distill}^{N_i}) \\ &= (L_{task}^S + \sum L_{task}^{N_i}) + (L_{distill}^S + \sum L_{distill}^{N_i}) \\ &= L_{task} + L_{distill} \end{aligned} \quad (18)$$

It should be noted that the primary objective of a stepping-stone is to achieve feature alignment. Instead of utilizing feature-distillation as described in Eq. 5, we propose a revised formulation for $L_{feature}$, as

$$\begin{aligned} L_{feature} &= \sum d_i^F(F_i^S, F_i^T) \\ &= \sum d^L(Y^{N_i}, Y^T) = \sum L_{distill}^{N_i} \end{aligned} \quad (19)$$

Moreover, as shown in Fig. 3, there is potential for further optimization of the framework with the incorporation of logits distillation between stepping models, denoted as L_{cross} , which could further enhance the overall effectiveness of the framework. We employ an ensemble to streamline its execution:

$$Y^{ensemble} = \frac{\sum_{i=1}^{i \leq n} Y^{N_i}}{n} \quad (20)$$

Then, the process of distillation between stepping stones is described as:

$$L_{cross} = d^L(Y^S, Y^{ensemble}) + \sum d^L(Y^{N_i}, Y^{ensemble}) \quad (21)$$

All in all, Fig. 3 presents the entire process of Block-KD very well. Compared with vallyna KD, in addition to obtaining the respective logits of student and teacher, we also obtained the logits of the intermediate state according to the calculation of stepping-stones, and integrated learning objectives with control hyperparameters α, β, γ :

$$L = \alpha L_{task} + \beta L_{distill} + \gamma L_{cross} \quad (22)$$

IV. THEORETICAL ANALYSIS

The improvements brought by the Block-KD framework to the student backbone can be analyzed from various perspectives.

First, let us show that distillation through stepping-stones effectively aligns intermediate features. Given two features that need to be aligned, F_i^T and F_i^S , we denote the difference between them as $d_i^F(F_i^S, F_i^T) = d^L(Y^{N_i}, Y^T)$ to measure their divergence. We now show how $d_i^F(F_i^T, F_i^S)$ facilitates the alignment of these features. In this context, consider d^L to be the KL divergence loss (Eq. 4). Regarding the K -classes logit, $Y_k^{N_i}$ of the distilled stepping-stone model and Y_k^T of

the teacher model, where k represents the class dimension, the gradient of the distillation loss is given by:

$$\frac{\partial d^L}{\partial Y_k^{N_i}} = \frac{1}{\tau} \left(\frac{e^{Y_k^{N_i}/\tau}}{\sum_j e^{Y_j^{N_i}/\tau}} - \frac{e^{Y_k^T/\tau}}{\sum_j e^{Y_j^T/\tau}} \right) \quad (23)$$

If the temperature τ is high compared to the magnitude of the logits, we can approximate:

$$\frac{\partial d^L}{\partial Y_k^{N_i}} \approx \frac{1}{\tau} \left(\frac{1 + Y_k^{N_i}/\tau}{K + \sum_j Y_j^{N_i}/\tau} - \frac{1 + Y_k^T/\tau}{K + \sum_j Y_j^T/\tau} \right) \quad (24)$$

Assuming the logits have been zero-meaned separately for each transfer case such that $\sum_j Y_j^{N_i} = \sum_j Y_j^T = 0$, we have:

$$\frac{\partial d^L}{\partial Y_k^{N_i}} \approx \frac{1}{\tau^2 K} (Y_k^{N_i} - Y_k^T) \quad (25)$$

At this juncture, let $C_i(F_i^S) = F_i^P$, given $Y^{N_i} = M_i^P(F_i^P)$ and $Y^T = M_i^P(F_i^T)$, we have:

$$\begin{aligned} \frac{\partial d^L}{\partial F_i^P} &= \sum_k \left(\frac{\partial d^L}{\partial Y_k^{N_i}} \frac{\partial Y_k^{N_i}}{\partial F_i^P} \right) \\ &\approx \frac{1}{\tau^2 K} (Y^{N_i} - Y^T)^\top \frac{\partial M_i^P}{\partial F_i^P} \\ &= \frac{1}{\tau^2 K} (M_i^P(F_i^P) - M_i^P(F_i^T))^\top \frac{\partial M_i^P}{\partial F_i^P} \end{aligned} \quad (26)$$

Then, with a linear approximation, assuming the model M_i^P is approximately linear near F_i^P , we can retain only the first-order term in Taylor expansion at F_i^P :

$$M_i^P(F_i^T) \approx M_i^P(F_i^P) + \frac{\partial M_i^P}{\partial F_i^P} (F_i^T - F_i^P) \quad (27)$$

Substituting this approximation into the original gradient expression, we obtain:

$$\frac{\partial d^L}{\partial F_i^P} \approx \frac{1}{\tau^2 K} \left(\frac{\partial M_i^P}{\partial F_i^P} (F_i^P - F_i^T) \right)^\top \frac{\partial M_i^P}{\partial F_i^P} \quad (28)$$

This gradient directly influences the alignment of F_i^P and F_i^S . In the gradient descent method, the direction of adjustment for F_i^P should be toward reducing the difference between F_i^P and F_i^S , and this is determined by the direction and magnitude of $\frac{\partial M_i^P}{\partial F_i^P}$.

Besides, the stepping models constructed during training provide a moderately performing model akin to an implicit teacher-assistance [34] mechanism. The theoretical analysis of performance enhancement by creating these intermediate models is discussed in [34]. This analysis is primarily based on VC theory [49] and its relevant applications in the field of knowledge distillation [32]. Consider an initial scenario wherein a student begins learning without prior knowledge. According to the principles outlined in VC theory [49], the classification error of a classifier f_s is decomposable in the following manner:

$$R(f_s) - R(f_r) \leq O\left(\frac{|F_s|_C}{n^{\alpha_{sr}}}\right) + \epsilon_{sr} \quad (29)$$

Here, $O(\cdot)$ symbolizes the estimation error associated with the statistical learning processes given a specified dataset size, while ϵ_{sr} delineates the approximation error reflective of the model's inherent capability. Within this framework, $f_r \in F_r$ represents the authentic (ground truth) target function, and $f_s \in F_s$ denotes the learner or student function. R specifies the error magnitude, $|\cdot|_C$ quantifies the function class capacity, n denotes the dataset size, and α_{sr} ranges between 1/2 to 1, indicating a learning rate which approaches 1/2 for more complex tasks and nears 1 for simpler tasks. Similarly, assuming $f_t \in F_t$ as the teacher function, we have:

$$R(f_t) - R(f_r) \leq O\left(\frac{|F_t|_C}{n^{\alpha_{tr}}}\right) + \epsilon_{tr} \quad (30)$$

where α_{tr} and ϵ_{tr} are correspondingly defined to encapsulate the learning dynamics when the teacher is educated from scratch. Building upon the groundwork established by [32], and assuming that training is conducted through pure distillation ($\lambda = 1$), we facilitate direct knowledge transfer from the teacher to the student, thereby establishing a baseline for knowledge distillation. From this baseline, we derive:

$$R(f_s) - R(f_t) \leq O\left(\frac{|F_s|_C}{n^{\alpha_{st}}}\right) + \epsilon_{st} \quad (31)$$

in which α_{st} and ϵ_{st} relate to the student's learning process from the teacher. [32] highlighted the necessity for $|F_t|_C$ to remain minimal to ensure that traditional knowledge distillation surpasses rudimentary learning processes. Furthermore, it is imperative to recognize that $\alpha_{sr} \leq \alpha_{st}$ and $\alpha_{sr} \leq \alpha_{tr}$, with a larger gap indicating a reduced rate of learning. Additionally, according to assumptions made by [16], $\epsilon_{tr} + \epsilon_{st} \leq \epsilon_{sr}$. This setup confirms effective knowledge distillation:

$$O\left(\frac{|F_t|_C}{n^{\alpha_{tr}}} + \frac{|F_s|_C}{n^{\alpha_{st}}}\right) + \epsilon_{tr} + \epsilon_{st} \leq O\left(\frac{|F_s|_C}{n^{\alpha_{sr}}}\right) + \epsilon_{sr} \quad (32)$$

This relationship suggests that the aggregate error bound in traditional distillation is less than or equal to that in scratch learning, valid asymptotically as $n \rightarrow \infty$. In scenarios where the sample size is finite and $|F_t|_C$ is excessively large, these inequalities might fail, indicating potential shortcomings in the distillation process. Another failure scenario for traditional knowledge distillation arises when there is a significant disparity in capacity between the student and teacher, particularly when α_{st} is minimal. Leveraging their insights and analytical framework, let us introduce an intermediate stepping-stone model, denoted as f_n , between the student and teacher:

$$R(f_s) - R(f_n) \leq O\left(\frac{|F_s|_C}{n^{\alpha_{sn}}}\right) + \epsilon_{sn} \quad (33)$$

and subsequently, this stepping-stone model assimilates knowledge from the teacher:

$$R(f_n) - R(f_t) \leq O\left(\frac{|F_n|_C}{n^{\alpha_{nt}}}\right) + \epsilon_{nt} \quad (34)$$

Here, α_{sn} , ϵ_{sn} , α_{nt} , and ϵ_{nt} are defined to elucidate the learning dynamics within this tripartite framework. It is pertinent to note that the incorporation of an intermediary simplifies the learning process, whether it is the student learning from

TABLE I

RESULTS OF TOP-1 ACCURACY (%) ON CIFAR-100 UNDER UNIFORM ARCHITECTURE. BLOCK[KD], BLOCK[DKD], AND BLOCK[MLKD] REFER TO PROPOSED BLOCK-WISE LOGIT DISTILLATION UNDER THE LOGIT OBJECTIVES OF CLASSICAL KD[16], DKD[65], AND MLKD[22] RESPECTIVELY. BLOCK[DKD][†] INDICATES THE LIGHT VERSION, UTILIZING THE LAST TWO STEPPING MODELS. * SIGNIFIES CONFIGURATIONS THAT INCLUDE DATA AUGMENTATION AND 480 TRAINING EPOCHS FOLLOWING MLKD[22]. ALL RESULTS ARE THE AVERAGE OVER 5 TRIALS.

Method	Teacher	ResNet56	ResNet110	ResNet32×4	WRN40-2	WRN40-2	VGG13
	Student	ResNet20	ResNet32	ResNet8×4	WRN16-2	WRN40-1	VGG8
		72.34	74.31	79.42	75.61	75.61	74.64
		69.06	71.14	72.50	73.26	71.98	70.36
Feature	FitNet [41]	69.21	71.06	73.50	73.58	72.24	71.02
	RKD [36]	69.61	71.82	71.90	73.35	72.22	71.48
	CRD [47]	71.16	73.48	75.51	75.48	74.14	73.94
	OFD [14]	70.98	73.23	74.95	75.24	74.33	73.95
	ReviewKD [5]	71.89	73.89	75.63	76.12	75.09	74.84
	FAM-KD [38]	72.15	74.45	76.84	76.47	75.40	/
w/ Logit	DML [64]	69.52	72.03	72.12	73.58	72.68	71.79
	TAKD [34]	70.83	73.37	73.81	75.12	73.78	73.23
	WSLD [66]	72.15	74.12	76.05	/	74.48	/
	WCoRD [4]	71.92	74.20	76.15	76.11	74.72	/
	NKD [59]	/	/	76.35	/	/	74.86
	CKD [62]	72.03	74.14	76.62	76.29	74.85	74.86
	KD [16]	70.66	73.08	73.33	74.92	73.54	72.98
	Block[KD]	71.71	73.95	76.26	75.67	74.83	74.54
	DKD [65]	71.97	74.11	76.32	76.24	74.81	74.68
	OFD+DKD	71.12	73.53	75.22	76.03	74.73	74.73
ReviewKD+DKD	71.63	74.20	76.01	76.15	74.86	74.96	
Block[DKD] [†]	72.06	74.15	77.18	76.26	75.14	75.06	
Block[DKD]	72.03	74.17	77.28	76.30	75.21	75.05	
MLKD* [22]	72.19	74.11	77.08	76.63	75.35	75.18	
Block[MLKD]*	72.43	74.72	77.84	76.76	75.97	75.34	

the intermediary or the intermediary from the teacher, i.e., $\alpha_{st} \leq \alpha_{sn}$ and $\alpha_{st} \leq \alpha_{nt}$, thus,

$$O\left(\frac{|F_n|_C}{n^{\alpha_{nt}}} + \frac{|F_s|_C}{n^{\alpha_{sn}}}\right) \leq O\left(\frac{|F_s|_C}{n^{\alpha_{st}}}\right) \quad (35)$$

Additionally, under the assumptions made by [16], $\epsilon_{nt} + \epsilon_{sn} \leq \epsilon_{st}$, we have,

$$O\left(\frac{|F_n|_C}{n^{\alpha_{nt}}} + \frac{|F_s|_C}{n^{\alpha_{sn}}}\right) + \epsilon_{nt} + \epsilon_{sn} \leq O\left(\frac{|F_t|_C}{n^{\alpha_{tr}}} + \frac{|F_s|_C}{n^{\alpha_{st}}}\right) + \epsilon_{st}, \quad (36)$$

These relationships corroborate that the upper bound of error with a stepping-stone model is smaller than in vanilla knowledge distillation. In scenarios characterized by significant performance disparities between the student and the teacher, the integration of a stepping-stone model intermediary effectively partitions the modest α_{st} into two more tractable components, α_{sn} and α_{nt} . This strategic division substantially enhances the efficiency of the knowledge distillation process, optimizing the learning trajectory for the student.

Moreover, the principles underlying Block-KD’s branch structure are reminiscent of self-distillation, and its benefits can be understood through a multi-view hypothesis [2]. Introducing L_{cross} , which averages votes during the training

process, often leads to more effective teaching labels. This approach aligns with constructing an output ensemble [51]. During training, it can yield performance that surpasses even the initial teacher model, thereby elevating the overall framework’s upper bound. These observations generally align with empirical experiments [51].

V. EXPERIMENTS

A. Experiments Details on Visual Tasks

1) *Datasets*: Three widely researched datasets are used in experiments: (1) CIFAR-100 [24], the well-known classification dataset of 32×32 images, with 50K training samples and 10K test samples for 100 classes; (2) ImageNet [42], the challenging large-scale classification dataset of high-resolution images, with 1.28M training samples and 50K test samples for 1000 classes; (3) MS-COCO [29], the general object detection dataset, with 118,000 training samples and 5,000 validation samples from 80 categories.

2) *Setting*: In our experiments, two primary conditions are addressed. 1) Uniform case in which both the teacher and student models have the same architectural design. 2) Non-uniform case in which the structures of the two models

TABLE II

RESULTS OF TOP-1 ACCURACY (%) ON CIFAR-100 UNDER NON-UNIFORM ARCHITECTURE. BLOCK[KD], BLOCK[DKD], AND BLOCK[MLKD] REFER TO PROPOSED BLOCK-WISE LOGIT DISTILLATION UNDER THE LOGIT OBJECTIVES OF CLASSICAL KD [16], DKD [65], AND MLKD [22] RESPECTIVELY. BLOCK[DKD][†] INDICATES THE LIGHT VERSION, UTILIZING THE LAST TWO STEPPING MODELS. * SIGNIFIES CONFIGURATIONS THAT INCLUDE DATA AUGMENTATION AND 480 TRAINING EPOCHS FOLLOWING MLKD [22]. ALL RESULTS ARE THE AVERAGE OVER 5 TRIALS.

Method	Teacher	ResNet32x4	WRN40-2	VGG13	ResNet50	ResNet32x4
	Student	ShuffleNetV1	ShuffleNetV1	MobileNetV2	MobileNetV2	ShuffleNetV2
		79.42	75.61	74.64	79.34	79.42
		70.50	70.50	64.60	64.60	71.82
Feature	FitNet [41]	73.59	73.73	64.14	63.16	73.54
	RKD [36]	72.28	72.21	64.52	64.43	73.21
	CRD [47]	75.11	76.05	69.73	69.11	75.65
	OFD [14]	75.98	75.85	69.48	69.04	76.82
	ReviewKD [5]	77.45	77.14	70.37	69.89	77.78
	FAM-KD [38]	77.76	77.57	70.88	/	78.41
	DML [64]	72.89	72.76	65.63	65.71	73.45
	TAKD [34]	74.53	75.34	67.91	68.02	74.82
	WSLD [66]	75.46	76.21	/	/	75.93
	WCoRD [4]	75.77	76.68	70.02	76.48	/
	NKD [59]	75.31	75.96	69.39	68.72	76.26
w/ Logit	KD [16]	74.07	74.83	67.37	67.35	74.45
	SDD+DKD [54]	76.30	76.65	68.79	69.55	76.67
	Block[KD]	77.51	76.82	69.33	71.42	77.52
	DKD [65]	76.45	76.70	69.71	70.35	77.07
	OFD+DKD	76.99	76.85	69.72	70.23	77.34
	ReviewKD+DKD	77.43	77.23	70.23	70.44	77.52
	SDD+DKD [54]	77.30	77.21	70.25	71.36	78.05
	Block[DKD] [†]	77.88	77.21	69.77	72.19	78.07
	Block[DKD]	78.12	77.26	69.82	72.24	78.35
	MLKD* [22]	77.18	77.44	70.57	71.04	78.44
	Block[MLKD]*	78.29	77.86	70.88	72.54	79.00

are distinct. We employ a variety of network architectures, including ResNet [12], WRN [61], VGG [45], ShuffleNet-V1/V2 [33, 63], and MobileNet-V1/V2 [18, 43]. We report the typical or recent methods of both feature and logit distillation for comparison: FitNet [41], RKD [36], CRD [47], OFD [14], ReviewKD [5], vallina KD [16], DML [64], TAKD [34], DKD [65], MLKD [22].

3) *Implementation Details*: Firstly, the positions of the feature-level distillation need to be determined. The term "block" refers to the traversed layers between distillation positions. We follow the standard block strategy of feature distillation [5, 14, 51], which typically involves dividing blocks based on their resolution prior to downsampling, consistent with the practice of convolutional architecture (e.g. 3-blocks or 4-blocks ResNet architecture). The objectives of the stepping stone, $\{L^{N_i}\}_{i \leq n}$, are divided by the coefficient 2^{n-i} , where n is the total number of blocks, in order to reconcile the correlation between step L^N and final L^S , thereby preventing overfitting on stepping-stones. Our framework employs the same connectors as OFD [14], which consist of a single 1x1 convolutional layer coupled with a batch normalization layer for channel combination. Then, our experimental implemen-

tation adheres to the standard strategy identified in previous works [5, 47, 65], specifically with regard to each dataset:

On CIFAR-100. Models are trained using SGD for 240 epochs with batch size of 64. The weight decay and momentum are set to $5e-4$ and 0.90, respectively. The learning rates for VGG, ResNet, and WRN students are 0.05, while those for ShuffleNet and MobileNet are 0.01. Using a multi-step schedule, the learning rate is divided by 10 at the 150, 180, and 210 epochs. The steady weight of all objectives, L_{task} , $L_{distill}$, and L_{cross} , is set to 1.0, and a 20-epoch linear warmup is used for $L_{distill}$ and L_{cross} . The hyperparameters within the logit distance, d^L , of both classical KD and DKD are set according to DKD's original paper [65], in which the temperature is set to 4 and the controlling factors on various architectures are altered.

On ImageNet. Following [5, 47, 65] to the letter, we train the models for 100 epochs with the batch size of 512, the learning rate of 0.2 divided by 10 every 30 epochs, and the weight decay of $1e-4$. We apply the same configuration of DKD loss [65], in which the inside hyperparameters of DKD, α_{DKD} and β_{DKD} , are set to 0.5, 0.5 for the uniform pair of ResNet-34 and ResNet-18 and to 0.5, 2.0 for the non-uniform

pair of ResNet-50 and MobileNet-V1. The steady weight of all objectives, L_{task} , $L_{distill}$, and L_{cross} , is set to 1.0 and a linear warmup is utilized for the adaptation of stepping-stones in the first 5 epochs.

On MS-COCO. Implementation follows the settings in [5]. We employ the two-stage method, Faster RCNN with FPN [30, 40] as the foundation. All students are trained with the 1x scheduler (using the identical schedulers and task-specific loss weights as in Detectron2 [56]). The backbone and FPN are viewed as a single complete block, and the connector used to transfer FPN output features employs ABF structure proposed in [5]. $L_{distill}$ and L_{cross} are defined on DKD with the same setting in [65].

All results of compared methods are reported in their original papers or reproduced by previous works [5, 47, 65].

B. Experiments Details on NLP tasks

1) *Datasets:* We have also extended the application of Block-KD to evaluate its performance across various benchmarks within the field of NLP: Microsoft Research Paraphrase Matching (MRPC) [10] and Quora Question Pairs (QQP) [44] are used for assessing paraphrase similarity; the Recognizing Textual Entailment (RTE) [3] task for natural language inference; and the Corpus of Linguistic Acceptability (CoLA) [53] for determining linguistic acceptability. Following [50], we use classification accuracy as the evaluation metric for the RTE datasets, both the accuracy and the F1 score for MRPC and QQP, and the Matthew’s correlation coefficient for CoLA.

2) *Settings:* For our experiments on NLP benchmarks, which entail sentence or sentence-pair classification tasks, we leverage the architecture from the original BERT model [8]. The standard configuration of the teacher model, referred to as BERT₁₂, includes 12 transformer layers, a hidden size of $d = 768$, a feedforward size of $d_i = 3072$, and $h = 12$ attention heads, totaling 109 million parameters. For the student models, we use BERT₄ (with $d = 312$, $d_i = 1200$, $h = 12$, and 14.5 million parameters) and BERT₆ (with $d = 768$, $d_i = 3072$, $h = 12$, and 67.0 million parameters). To enable effective knowledge distillation, the teacher model is pre-finetuned for each task [46], and the student models are initialized with a generalized distillation strategy derived from [21, 26].

3) *Implementation Details:* During the distillation phase, the teacher model supplies logits as soft labels for the students, employing a standard KL divergence loss (Eq. 4) for distillation. Training involves 10 epochs of fine-tuning with a batch size of 32, a learning rate of 2×10^{-5} , and distillation coefficients $\alpha = 0.2$, $\beta = 0.8$ in Eq. 6, with $\tau = 1.0$ in Eq. 4 for tasks of CoLA, MRPC, and QQP. For the RTE task, coefficients are adjusted to $\alpha = \beta = 0.5$ and $\tau = 3.0$. Within the Block-KD framework, for simplicity, BERT’s embeddings and encoder are treated as a single block and the classifier as a replaceable block, facilitating a lightweight framework verification test. At this stage, only one stepping-stone is created, merging the student’s embeddings and encoder with the teacher’s classifier, with a linear connector placed between the student’s encoder and the teacher’s classifier. In this simplified setup, L_{cross} is not activated.

TABLE III
RESULTS OF TOP-1 AND TOP-5 ACCURACY (%) ON THE IMAGENET VALIDATION. TEACHER-STUDENT PAIRS ARE RESNET-34/RESNET-18 AND RESNET-50/MOBILENET-V1 FOR UNIFORM AND NON-UNIFORM ARCHITECTURE, RESPECTIVELY.

		Top-1	Top-5	Top-1	Top-5
Method	Teacher	ResNet34 73.31	91.42	ResNet50 76.16	92.86
	Student	ResNet18 69.75	89.07	MobileNet-V2 68.87	88.76
Feature	AT [60]	70.69	90.01	69.56	89.33
	OFD [14]	70.81	89.98	71.25	90.34
	CRD [47]	71.17	90.13	71.37	90.41
	WCoRD [4]	71.49	90.16	/	/
	ReviewKD [5]	71.61	90.51	72.56	91.00
	MGD [58]	71.58	90.35	72.35	90.71
Logit	KD [16]	71.03	90.05	70.50	89.80
	DML [64]	70.82	90.02	71.35	90.31
	WSLD [66]	71.54	90.25	72.02	90.70
	DKD [65]	71.70	90.41	72.05	91.05
	NKD [59]	71.96	/	72.58	/
Feature + Logit	SRRL [57]	71.73	90.60	72.49	90.92
	MGD+WSLD [58]	71.80	90.40	72.59	90.94
	CKD [62]	71.79	90.58	/	/
	Block[DKD]	72.26	90.76	73.11	91.33

C. Main Results

Results on CIFAR-100 image classification. Tab. I and Tab. II show the performance of various distillation schemes under both uniform and non-uniform architectures. To implement the objectives of Block-KD (Eq. 22), we employ the logit-based distance (d^L) suggested by vallina KD and DKD, respectively. Notably, with the Block-KD framework, the logit-based scheme is capable of achieving consistent development. The Block-KD based on vallina KD has been able to outperform complex feature methods in the majority of instances, and the scheme with DKD has yielded the best results in nearly all cases. On this basis, the lightweight version with only the last two stepping models reduces computational costs to levels comparable to OFD and ReviewKD for comparison (see Block[DKD][†] in Tab. I and Tab. II). We also conduct experiments with combinations of feature-based OFD, ReviewKD, and logit-based DKD in Tab. I and Tab. II. Notably, the results of combined methods tend to fall between the individual performance levels of feature and logit methods. This suggests that the training objectives of logits and features may diverge, a phenomenon consistent with related experiments in [47]. While in specific limited application scenarios, block-KD delivers stable performance improvements over logit methods, which underscores the advantages of block-KD compared to feature methods.

Results on ImageNet image classification. Tab. III illustrates the distillation results on the large-scale task with both Top-1 and Top-5 accuracies, demonstrating that our method still outperforms the state-of-the-art distillation methods on such a large and complex dataset. Notably, the logit distillation method DKD and the feature distillation method ReviewKD have advantages in different indices, whereas our proposed block-wise logit distillation has completely surpassed them.

Results on MS-COCO object detection. To verify the

TABLE IV

RESULTS ON MS-COCO BASED ON FASTER-RCNN-FPN WITH AP EVALUATED ON VAL2017. TEACHER-STUDENT PAIRS ARE RESNET-101 (R-101) & RESNET-18 (R-18), RESNET-101 & RESNET-50 (R-50) AND RESNET-50 & MOBILENET-V2 (MV2).

		R101 & R-18			R101 & R-50			R50 & R-MV2		
		AP	AP ₅₀	AP ₇₅	AP	AP ₅₀	AP ₇₅	AP	AP ₅₀	AP ₇₅
Method	teacher	42.04	62.48	45.88	42.04	62.48	45.88	40.22	61.02	43.81
	student	33.26	53.61	35.26	37.93	58.84	41.05	29.47	48.87	30.90
Feature	FitNet [41]	34.13	54.16	36.71	38.76	59.62	41.80	30.20	49.80	31.69
	FGFI [52]	35.44	55.51	38.17	39.44	60.27	43.04	31.16	50.68	32.92
	ReviewKD [5]	36.75	56.72	34.00	40.36	60.97	44.08	33.71	53.15	36.13
Logit	KD [16]	33.97	54.66	36.62	38.35	59.41	41.71	30.13	50.28	31.35
	DKD [65]	35.05	56.60	37.54	39.25	60.90	42.73	32.34	53.77	34.01
	Block[DKD]	36.32	57.30	38.97	40.34	61.47	43.79	34.45	54.76	36.82

TABLE V

RESULTS ON NLP TASKS WITH BERT MODELS. THE MODELS ARE EVALUATED ON DATASETS OF MRPC, QQP, RTE, AND CoLA, RESPECTIVELY.

	MRPC (Acc/F1)	QQP (Acc/F1)	RTE (Acc)	CoLA (Correlation)
BERT ₄	82.11/87.69	86.97/82.73	65.70	18.50
w/ vanilla KD	85.05/89.54	87.82/83.85	66.43	20.55
w/ Block-KD	86.52/90.73	89.20/85.47	68.23	22.65
BERT ₆	86.03/90.09	89.54/85.93	71.84	20.72
w/ vanilla KD	87.01/90.94	89.95/86.39	72.20	41.30
w/ Block-KD	87.25/91.13	90.56/87.30	73.29	45.04

generality of the Block-KD method, we applied it to the object detection task. Faster-RCNN-FPN [30, 40] serves as the foundation, while AP, AP50, and AP75 are used for the evaluation metric. The Block-KD framework needs to be extended to match the FPN structure in this case. The backbone and FPN are seen as one complete block. The connector is used to transfer FPN output features from the student to the teacher. The teacher ROI generates intermediate logits and instructed logits based on the proposals from the student RPN module, using both student-transferred features and raw features. The distillation goal of Block-KD can then be defined using those step logits and the student’s ROI output. Since the output of FPN is a compilation of several features, which limits the use of the simple convolution structure as in classification tasks, the ABF proposed in ReviewKD [5] is employed as the connector portion for feature alignment.

Results for BERT Models on NLP Tasks. Tab. V presents the distillation outcomes for BERT models across four NLP tasks. Unlike in visual tasks, the Block-KD framework incorporates only one intermediary stepping-stone model in this context, and involves minimal additional overhead—just the teacher’s classifier and a linear connector. This streamlined setup is designed to validate the method’s generalizability. Observations indicate that employing a distillation loss, alongside training the student model with hard targets, can moderately enhance performance. Furthermore, the Block-KD framework seems to amplify these benefits, enhancing the efficacy of the

TABLE VI

COMPARISON OF DIFFERENT IMPLEMENTATIONS IN FEATURE ALIGNMENT. RESNET32x4 AND RESNET8x4 ARE PAIRED ON CIFAR-100. THE EXPERIMENTAL RESULTS ARE DETERMINED UNDER TWO CONDITIONS: 1) ONLY FEATURE-BASED OBJECTIVE, $L_{feature}$ IS USED TO ACHIEVE FEATURE ALIGNMENT, IN ACCORDANCE WITH THE SCHEMES PROPOSED IN EACH WORK. 2) BASED ON $L_{feature}$, ADDITIONALLY DEFINE A LOGIT-BASED OBJECTIVE, L_{logit} , THAT FOLLOWS THE STANDARD KD LOSS (EQ. 4) FOR OUTPUT LOGITS.

Mechanism	Method	Top-1 Acc (%)	
		$L_{feature}$	w/ L_{logit}
None	Baseline	72.50	73.33
Alignment via Projected Features	AT [60]	73.44	74.53
	FT [23]	72.86	74.62
	VID [1]	73.09	74.56
Direct Alignment on Raw Features	FitNets [41]	73.50	74.66
	AB [15]	73.17	74.40
	OFD [14]	74.95	75.27
Alignment via Block-wise Logits	Block	75.41	75.94

distillation process. Consequently, our method remains well-suited for transformer architectures and is effective across various applications within the NLP domain, showcasing the framework’s adaptability and broad applicability.

D. Analysis and Discussion

Comparison of Feature Alignment Implementations. Tab. VI compares various feature alignment implementations. On the premise of implementing feature alignment, it is discovered that all feature-based methods can define additional logit-based objectives on output to achieve positive results. This demonstrates that feature alignment is possible within a logit-based scheme and that the two are not mutually exclusive. Notably, the OFD connector is also a single-layer 1x1 convolution, which is consistent with our connector design. This connection method is lightweight and only considers the linear connection on the channel to align the dimension of the feature, allowing for high scalability. Based

TABLE VII
ABLATION STUDY OF TRAINING OBJECTIVES (EQ. 22). RESNET32x4
AND RESNET8x4 ARE PAIRED ON CIFAR-100.

L^S		L^N			Top-1 (%)
L^S_{task}	$L^S_{distill}$	L^N_{task}	$L^N_{distill}$	L_{cross}	
✓					72.50
✓	✓				73.33
✓		✓			74.09
✓			✓		75.41
✓	✓	✓			75.31
✓	✓		✓		75.94
✓	✓	✓	✓		76.15
✓	✓	✓		✓	76.16
✓	✓	✓	✓	✓	76.26

on the consistent connector structure, the comparison between Block and OFD can exactly reflect the increase of unified feature alignments (Fig. 2c) over direct alignment (Fig. 2b), indicating the source of our scheme’s benefits. Compared to other feature alignment schemes, our scheme obtains the best results, demonstrating that the proposed implicit feature alignment via logits is meaningful, and it allows for further investigation into the potential of feature alignment.

Ablation Study of Training Objectives. Experiments involving the ablation of training objectives are conducted, with the ablation components being added sequentially to determine their effects. The results are summarized in Tab. VII. Vallina KD is applied to the logit distance d^L for $L^S_{distill}$, $L^N_{distill}$, and L_{cross} in this experiment. The original student objectives utilized in the logit-based distillation methods, L^S_{task} and $L^S_{distill}$, are defined based on the classification targets and the teacher’s soft labels (Eq. 6). The objectives of the stepping stones, denoted L^N_{task} , $L^N_{distill}$, and L_{cross} , are defined by classification targets, teacher logits, and preceding step logits. It can be found that $L^N_{distill}$ has a significant performance improvement when used in conjunction with other objectives, indicating that our implementation of logit-based feature alignment is practical and effective. In addition, introducing L^N_{task} can further enhance performance based on $L^N_{distill}$, demonstrating that the definition of task training objectives for stepping-stone can aid in the general functioning of the distillation framework. Furthermore, the expected improvement in overall performance can be realized by incorporating the logit distillation between phases, L_{cross} . All objectives have contributed positively to the distillation framework and are compatible with one another.

Discussion on Loss Combinations The purpose of L^N_{task} is to guide the stepping models towards task convergence, thereby facilitating collaborative work of S ’s blocks and connectors with T ’s blocks. Building upon this, $L^N_{distill}$ enhances stepping models and achieves feature alignment in the latent logits space. L_{cross} leverages ensemble learning to derive superior soft labels, elevating the overall performance. The visualized results align with our expectations (Fig. 4b). Adding $L^N_{distill}$ enhances branch training, improving S and N_2 (green to blue). Incorporating L_{cross} at the 200th epoch further extends the

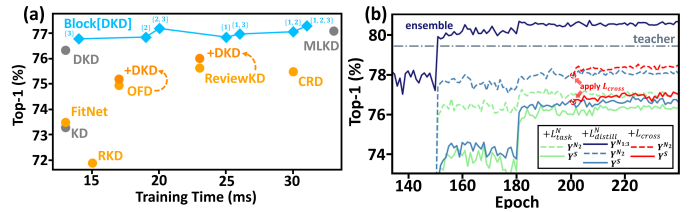


Fig. 4. Visualization Results with the R32x4 & R8x4 Pair on CIFAR-100. (a) Cost comparison. (b) Validation results during training. The green line represents results obtained by adding L^N_{task} to the baseline; the blue line further adds $L^N_{distill}$; and the red line incorporates L_{cross} at the 200th epoch upon the blue line.

TABLE VIII
COMPARISON OF TRAINING COSTS UNDER DIFFERENT SCHEMES.
RESNET32x4 AND RESNET8x4 ARE PAIRED ON CIFAR-100. THREE
INDICATORS OF CONCERN IN THE TRAINING PHASE ARE LISTED:
AUXILIARY PARAMETERS (MB), TRAINING DURATION (MILLISECONDS
PER BATCH), AND TOP-1 ACCURACY (%).

	Time (ms)	Params (MB)	Top-1 (%)
KD [16]	13	0	73.33
FitNet [41]	13	0.065	73.50
RKD [36]	15	0	71.90
CRD [47]	30	49.06	75.48
OFD [14]	17	0.332	74.95
ReviewKD [5]	23	6.87	75.63
DKD [65]	13	0	76.32
Block[DKD]†	20	0.315	77.18
Block[DKD]	31	0.332	77.28

performance boundary (blue to red).

Training Overhead. Tab. VIII contrasts the training costs of various methods. All feature-based methods must contain additional parameters to coordinate the teacher and the student; since our framework only requires the extension of connectors, the number of parameters is relatively modest. Due to the necessity of projecting the alignment features into the logit space, the training speed is slowed. Block-KD has similar training costs to CRD (Fig. 4a). However, a simple method can be employed to reduce the computational complexity by decreasing the required number of stepping stones (see Block[DKD]† in Tab. I and Tab. II), which may be considered to optimize deployment; the discussion is included in the following section.

Pruning Stepping-stones. The implicit computation of stepping-stones increases training costs since features must be projected into the logits space through the teacher’s back-end feature extraction blocks. The core goal of knowledge distillation is to produce a lightweight model so that training costs can be accepted to some extent [51]. Despite the fact that this issue is not critical, we consider mitigating it to illustrate the optimization field and application value of block-wise logit distillation. Note that all the initial stepping-stones are utilized to ensure the one-to-one correspondence between blocks; however, this restriction may be excessively stringent. Therefore, as an optimization strategy, it makes sense to consider reducing the quantity of stepping stones. The outcomes of our experiments to prune stepping-stones on the resnet32x4/resnet32x8 pair are shown in Tab. IX. For the pair

TABLE IX

COMPARISON OF TRAINING COSTS UNDER DIFFERENT SETTINGS OF STEPPING-STONES. RESNET32×4 AND RESNET8×4 ARE PAIRED ON CIFAR-100. THE BASE REFERS TO DKD [65], WHERE STEPPING-STONES N_1 , N_2 , AND N_3 ARE ADDED GRADUALLY FOR PERFORMANCE ENHANCEMENT. THREE INDICATORS OF CONCERN IN THE TRAINING PHASE ARE LISTED: AUXILIARY PARAMETERS (MB), TRAINING DURATION (MILLISECONDS PER BATCH), AND TOP-1 ACCURACY (%).

	Time (ms)	Params (MB)	Top-1 (%)
base	13	0	76.32
w/ N_1	25	0.0161	76.84
w/ N_2	19	0.0635	76.84
w/ N_3	14	0.2520	76.77
w/ N_1, N_2	30	0.0796	77.05
w/ N_1, N_3	26	0.2681	76.96
w/ N_2, N_3	20	0.3154	77.18
w/ N_1, N_2, N_3	31	0.3315	77.28

composed of resnet32×4 and resnet8×4, it is divided into three blocks during distillation; therefore, three stepping-stones are used to determine logits at this time, which are recorded as N_1 , N_2 , and N_3 . Pruning on stepping-stones reveals that N_1 has a major impact on computing time, but that only a small number of parameters need to be introduced. This is primarily because the number of shallow channels is small, and thus the input and output dimensions of the connector are relatively smaller. However, the calculation of N_1 must traverse nearly all of T 's blocks, nearly doubling the calculation time. N_3 has the largest effect on the number of implemented parameters, but its additional calculation time is negligible, as expected. The calculation of N_3 is equivalent to leasing T 's classification to S , thus the calculation cost is very low; however, due to the large number of channels, the number of introduced parameters is the highest. N_3 performs marginally worse when only a single stepping-stone is used, while N_1 and N_2 perform similarly, and N_2 is recommended due to its faster processing speed. In the case of two stepping stones, the combination of N_2 and N_3 achieves the highest performance and the fastest calculation speed. In conclusion, the middle stepping stone is recommended first when selecting stepping stones; shallow stepping stones (with smaller i) can be appropriately discarded when training time is a factor, and deep stepping stones (with larger i) can be appropriately discarded when the number of auxiliary parameters is a factor.

Why does L_{cross} improve the Block-KD? L_{cross} is a further optimization of logit-based feature alignment, which is simply extended within the framework of block-wise logit distillation in practice. The benefits it provides can be viewed from two perspectives. At first, the concept of ensemble learning may be introduced, in which stepping-stone models are regarded as separate students. Therefore, the knowledge acquired by all students can effectively guide each student to enhance their learning outcomes. This concept is known as student collaboration. Second, using the output of a previous stepping-stone as the target for a subsequent stepping model is consistent with the intuitive notion of feature alignment, where the focus of alignment has shifted away from the front-end student block and teacher block (that is, alignment between blocks

$\{T_1, \dots, T_i\}$ and $\{S_1, \dots, S_i\}$, when T and N_i are paired). Instead, when the same student block is positioned at the front, there is a desire to align both the student's blocks and teacher's blocks in the middle (say, alignment between blocks $\{T_{i+1}, \dots, T_k\}$ and $\{S_{i+1}, \dots, S_k\}$, when N_i and N_k are paired), which represents an enhanced version of the original feature alignment.

Potential Biases and Ethical Implications. In the Block-KD framework, while knowledge distillation from a teacher model to a student model generally enhances performance, it is worth noting some subtle nuances. There could be a slight potential for the student model to inherit biases present in the teacher model, simply because it learns not only the explicit task at hand but also deeper patterns that may not be immediately evident. Additionally, the implicit nature of knowledge transfer through logit and feature alignment might make it a bit challenging to fully trace decision-making processes within the student model, which could be relevant in scenarios where understanding the basis of decisions is important. As a precautionary measure, while not dominant, ensuring that the distilled model performs fairly across various groups does merit attention. It's also sensible to consider the source of the distilled knowledge; the teacher model's quality can subtly influence the ethical standing of the student model. If the teacher model has not been thoroughly evaluated for potential ethical concerns, there's a slight chance that some of these might carry over to the student model.

VI. CONCLUSION

This paper shows the potential of integrating logit and features. Focusing on two mainstream types in knowledge distillation, feature- and logit-based methods, we reveal that the essential distinction between the two is their explicit prior alignment to "dark knowledge". This work provides a novel perspective on feature alignment to interpret the underlying differences between logit and feature distillation, and extends the standard implementations to achieve feature alignment in logits space. Furthermore, this work proposes a new distillation framework called block-wise logit distillation (Block-KD), which implements the alignment of feature-level "dark knowledge" based on the unified logit-based distillation with intermediate step logits generated by implicit stepping-stones. We hope this study will inspire future research to explore KD from a broader, more comprehensive vantage perspective, utilizing both logits and features.

REFERENCES

- [1] Sungsoo Ahn, Shell Xu Hu, Andreas Damianou, Neil D Lawrence, and Zhenwen Dai. Variational information distillation for knowledge transfer. In *Proceedings of the IEEE/CVF conference on computer vision and pattern recognition*, pages 9163–9171, 2019.
- [2] Zeyuan Allen-Zhu and Yuanzhi Li. Towards understanding ensemble, knowledge distillation and self-distillation in deep learning. *arXiv preprint arXiv:2012.09816*, 2020.
- [3] Luisa Bentivogli, Peter Clark, Ido Dagan, and Danilo Giampiccolo. The fifth pascal recognizing textual entailment challenge. *TAC*, 7(8):1, 2009.

- [4] Liqun Chen, Dong Wang, Zhe Gan, Jingjing Liu, Ricardo Henao, and Lawrence Carin. Wasserstein contrastive representation distillation. In *Proceedings of the IEEE/CVF conference on computer vision and pattern recognition*, pages 16296–16305, 2021.
- [5] Pengguang Chen, Shu Liu, Hengshuang Zhao, and Jiaya Jia. Distilling knowledge via knowledge review. In *Proceedings of the IEEE/CVF Conference on Computer Vision and Pattern Recognition*, pages 5008–5017, 2021.
- [6] Xu Cheng, Zhefan Rao, Yilan Chen, and Quanshi Zhang. Explaining knowledge distillation by quantifying the knowledge. In *Proceedings of the IEEE/CVF conference on computer vision and pattern recognition*, pages 12925–12935, 2020.
- [7] Jiequan Cui, Pengguang Chen, Ruiyu Li, Shu Liu, Xiaoyong Shen, and Jiaya Jia. Fast and practical neural architecture search. In *Proceedings of the IEEE/CVF international conference on computer vision*, pages 6509–6518, 2019.
- [8] Jacob Devlin. Bert: Pre-training of deep bidirectional transformers for language understanding. *arXiv preprint arXiv:1810.04805*, 2018.
- [9] Jacob Devlin, Ming-Wei Chang, Kenton Lee, and Kristina Toutanova. Bert: Pre-training of deep bidirectional transformers for language understanding. *arXiv preprint arXiv:1810.04805*, 2018.
- [10] Bill Dolan and Chris Brockett. Automatically constructing a corpus of sentential paraphrases. In *Third international workshop on paraphrasing (IWP2005)*, 2005.
- [11] Jonathan Frankle and Michael Carbin. The lottery ticket hypothesis: Finding sparse, trainable neural networks. *arXiv preprint arXiv:1803.03635*, 2018.
- [12] Kaiming He, Xiangyu Zhang, Shaoqing Ren, and Jian Sun. Deep residual learning for image recognition. In *Proceedings of the IEEE conference on computer vision and pattern recognition*, pages 770–778, 2016.
- [13] Kaiming He, Georgia Gkioxari, Piotr Dollár, and Ross Girshick. Mask r-cnn. In *Proceedings of the IEEE international conference on computer vision*, pages 2961–2969, 2017.
- [14] Byeongho Heo, Jeessoo Kim, Sangdoon Yun, Hyojin Park, Nojun Kwak, and Jin Young Choi. A comprehensive overhaul of feature distillation. In *Proceedings of the IEEE/CVF International Conference on Computer Vision*, pages 1921–1930, 2019.
- [15] Byeongho Heo, Minsik Lee, Sangdoon Yun, and Jin Young Choi. Knowledge transfer via distillation of activation boundaries formed by hidden neurons. *33(01):3779–3787*, 2019.
- [16] Geoffrey Hinton, Oriol Vinyals, and Jeff Dean. Distilling the knowledge in a neural network. *arXiv preprint arXiv:1503.02531*, 2015.
- [17] Andrew Howard, Mark Sandler, Grace Chu, Liang-Chieh Chen, Bo Chen, Mingxing Tan, Weijun Wang, Yukun Zhu, Ruoming Pang, Vijay Vasudevan, et al. Searching for mobilenetv3. In *Proceedings of the IEEE/CVF international conference on computer vision*, pages 1314–1324, 2019.
- [18] Andrew G Howard, Menglong Zhu, Bo Chen, Dmitry Kalenichenko, Weijun Wang, Tobias Weyand, Marco Andreetto, and Hartwig Adam. Mobilenets: Efficient convolutional neural networks for mobile vision applications. *arXiv preprint arXiv:1704.04861*, 2017.
- [19] Gao Huang, Zhuang Liu, Laurens Van Der Maaten, and Kilian Q Weinberger. Densely connected convolutional networks. In *Proceedings of the IEEE conference on computer vision and pattern recognition*, pages 4700–4708, 2017.
- [20] Benoit Jacob, Skirmantas Kligys, Bo Chen, Menglong Zhu, Matthew Tang, Andrew Howard, Hartwig Adam, and Dmitry Kalenichenko. Quantization and training of neural networks for efficient integer-arithmetic-only inference. In *Proceedings of the IEEE conference on computer vision and pattern recognition*, pages 2704–2713, 2018.
- [21] Xiaoqi Jiao, Yichun Yin, Lifeng Shang, Xin Jiang, Xiao Chen, Linlin Li, Fang Wang, and Qun Liu. Tinybert: Distilling bert for natural language understanding. *arXiv preprint arXiv:1909.10351*, 2019.
- [22] Ying Jin, Jiaqi Wang, and Dahua Lin. Multi-level logit distillation. In *Proceedings of the IEEE/CVF Conference on Computer Vision and Pattern Recognition*, pages 24276–24285, 2023.
- [23] Jangho Kim, SeongUk Park, and Nojun Kwak. Paraphrasing complex network: Network compression via factor transfer. volume 31, 2018.
- [24] Alex Krizhevsky, Geoffrey Hinton, et al. Learning multiple layers of features from tiny images. 2009.
- [25] Hao Li, Asim Kadav, Igor Durdanovic, Hanan Samet, and Hans Peter Graf. Pruning filters for efficient convnets. *arXiv preprint arXiv:1608.08710*, 2016.
- [26] Jianquan Li, Xiaokang Liu, Honghong Zhao, Ruifeng Xu, Min Yang, and Yaohong Jin. Bert-emd: Many-to-many layer mapping for bert compression with earth mover’s distance. *arXiv preprint arXiv:2010.06133*, 2020.
- [27] Quanquan Li, Shengying Jin, and Junjie Yan. Mimicking very efficient network for object detection. In *Proceedings of the IEEE conference on computer vision and pattern recognition*, pages 6356–6364, 2017.
- [28] Zheng Li, Jingwen Ye, Mingli Song, Ying Huang, and Zhigeng Pan. Online knowledge distillation for efficient pose estimation. In *Proceedings of the IEEE/CVF international conference on computer vision*, pages 11740–11750, 2021.
- [29] Tsung-Yi Lin, Michael Maire, Serge Belongie, James Hays, Pietro Perona, Deva Ramanan, Piotr Dollár, and C Lawrence Zitnick. Microsoft coco: Common objects in context. In *Computer Vision—ECCV 2014: 13th European Conference, Zurich, Switzerland, September 6–12, 2014, Proceedings, Part V 13*, pages 740–755. Springer, 2014.
- [30] Tsung-Yi Lin, Piotr Dollár, Ross Girshick, Kaiming He, Bharath Hariharan, and Serge Belongie. Feature pyramid networks for object detection. In *Proceedings of the IEEE conference on computer vision and pattern recognition*, pages 2117–2125, 2017.

- [31] Zhuang Liu, Mingjie Sun, Tinghui Zhou, Gao Huang, and Trevor Darrell. Rethinking the value of network pruning. *arXiv preprint arXiv:1810.05270*, 2018.
- [32] David Lopez-Paz, Léon Bottou, Bernhard Schölkopf, and Vladimir Vapnik. Unifying distillation and privileged information. *arXiv preprint arXiv:1511.03643*, 2015.
- [33] Ningning Ma, Xiangyu Zhang, Hai-Tao Zheng, and Jian Sun. Shufflenet v2: Practical guidelines for efficient cnn architecture design. In *Proceedings of the European conference on computer vision (ECCV)*, pages 116–131, 2018.
- [34] Seyed Iman Mirzadeh, Mehrdad Farajtabar, Ang Li, Nir Levine, Akihiro Matsukawa, and Hassan Ghasemzadeh. Improved knowledge distillation via teacher assistant. In *Proceedings of the AAAI conference on artificial intelligence*, volume 34, pages 5191–5198, 2020.
- [35] Daniel W Otter, Julian R Medina, and Jugal K Kalita. A survey of the usages of deep learning for natural language processing. *IEEE transactions on neural networks and learning systems*, 32(2):604–624, 2020.
- [36] Wonpyo Park, Dongju Kim, Yan Lu, and Minsu Cho. Relational knowledge distillation. In *Proceedings of the IEEE/CVF conference on computer vision and pattern recognition*, pages 3967–3976, 2019.
- [37] Baoyun Peng, Xiao Jin, Jiaheng Liu, Dongsheng Li, Yichao Wu, Yu Liu, Shunfeng Zhou, and Zhaoning Zhang. Correlation congruence for knowledge distillation. In *Proceedings of the IEEE/CVF International Conference on Computer Vision*, pages 5007–5016, 2019.
- [38] Cuong Pham, Van-Anh Nguyen, Trung Le, Dinh Phung, Gustavo Carneiro, and Thanh-Toan Do. Frequency attention for knowledge distillation. In *Proceedings of the IEEE/CVF Winter Conference on Applications of Computer Vision*, pages 2277–2286, 2024.
- [39] Mary Phuong and Christoph Lampert. Towards understanding knowledge distillation. In *International conference on machine learning*, pages 5142–5151. PMLR, 2019.
- [40] Shaoqing Ren, Kaiming He, Ross Girshick, and Jian Sun. Faster r-cnn: Towards real-time object detection with region proposal networks. volume 28, 2015.
- [41] Adriana Romero, Nicolas Ballas, Samira Ebrahimi Kahou, Antoine Chassang, Carlo Gatta, and Yoshua Bengio. Fitnets: Hints for thin deep nets. *arXiv preprint arXiv:1412.6550*, 2014.
- [42] Olga Russakovsky, Jia Deng, Hao Su, Jonathan Krause, Sanjeev Satheesh, Sean Ma, Zhiheng Huang, Andrej Karpathy, Aditya Khosla, Michael Bernstein, et al. Imagenet large scale visual recognition challenge. *International journal of computer vision*, 115:211–252, 2015.
- [43] Mark Sandler, Andrew Howard, Menglong Zhu, Andrey Zhmoginov, and Liang-Chieh Chen. Mobilenetv2: Inverted residuals and linear bottlenecks. In *Proceedings of the IEEE conference on computer vision and pattern recognition*, pages 4510–4520, 2018.
- [44] Lakshay Sharma, Laura Graesser, Nikita Nangia, and Utku Evci. Natural language understanding with the quora question pairs dataset. *arXiv preprint arXiv:1907.01041*, 2019.
- [45] Karen Simonyan and Andrew Zisserman. Very deep convolutional networks for large-scale image recognition. *arXiv preprint arXiv:1409.1556*, 2014.
- [46] Siqi Sun, Yu Cheng, Zhe Gan, and Jingjing Liu. Patient knowledge distillation for bert model compression. *arXiv preprint arXiv:1908.09355*, 2019.
- [47] Yonglong Tian, Dilip Krishnan, and Phillip Isola. Contrastive representation distillation. *arXiv preprint arXiv:1910.10699*, 2019.
- [48] Frederick Tung and Greg Mori. Similarity-preserving knowledge distillation. In *Proceedings of the IEEE/CVF international conference on computer vision*, pages 1365–1374, 2019.
- [49] Vladimir N Vapnik. An overview of statistical learning theory. *IEEE transactions on neural networks*, 10(5): 988–999, 1999.
- [50] Alex Wang. Glue: A multi-task benchmark and analysis platform for natural language understanding. *arXiv preprint arXiv:1804.07461*, 2018.
- [51] Lin Wang and Kuk-Jin Yoon. Knowledge distillation and student-teacher learning for visual intelligence: A review and new outlooks. *IEEE transactions on pattern analysis and machine intelligence*, 44(6):3048–3068, 2021.
- [52] Tao Wang, Li Yuan, Xiaopeng Zhang, and Jiashi Feng. Distilling object detectors with fine-grained feature imitation. In *Proceedings of the IEEE/CVF Conference on Computer Vision and Pattern Recognition*, pages 4933–4942, 2019.
- [53] A Warstadt. Neural network acceptability judgments. *arXiv preprint arXiv:1805.12471*, 2019.
- [54] Shicai Wei, Chunbo Luo, and Yang Luo. Scaled decoupled distillation. In *Proceedings of the IEEE/CVF Conference on Computer Vision and Pattern Recognition*, pages 15975–15983, 2024.
- [55] Yi Wei, Xinyu Pan, Hongwei Qin, Wanli Ouyang, and Junjie Yan. Quantization mimic: Towards very tiny cnn for object detection. In *Proceedings of the European conference on computer vision (ECCV)*, pages 267–283, 2018.
- [56] Yuxin Wu, Alexander Kirillov, Francisco Massa, Wan-Yen Lo, and Ross Girshick. Detectron2. <https://github.com/facebookresearch/detectron2>, 2019.
- [57] Jing Yang, Brais Martinez, Adrian Bulat, Georgios Tzimiropoulos, et al. Knowledge distillation via softmax regression representation learning. In *International Conference on Learning Representations*, 2021.
- [58] Zhendong Yang, Zhe Li, Mingqi Shao, Dachuan Shi, Zehuan Yuan, and Chun Yuan. Masked generative distillation. In *European Conference on Computer Vision*, pages 53–69. Springer, 2022.
- [59] Zhendong Yang, Ailing Zeng, Zhe Li, Tianke Zhang, Chun Yuan, and Yu Li. From knowledge distillation to self-knowledge distillation: A unified approach with normalized loss and customized soft labels. In *Proceedings of the IEEE/CVF International Conference on Computer Vision*, pages 17185–17194, 2023.
- [60] Sergey Zagoruyko and Nikos Komodakis. Paying more

- attention to attention: Improving the performance of convolutional neural networks via attention transfer. *arXiv preprint arXiv:1612.03928*, 2016.
- [61] Sergey Zagoruyko and Nikos Komodakis. Wide residual networks. *arXiv preprint arXiv:1605.07146*, 2016.
- [62] Weiwei Zhang, Yufeng Guo, Junhuang Wang, Jianqing Zhu, and Huanqiang Zeng. Collaborative knowledge distillation. *IEEE Transactions on Circuits and Systems for Video Technology*, 2024.
- [63] Xiangyu Zhang, Xinyu Zhou, Mengxiao Lin, and Jian Sun. Shufflenet: An extremely efficient convolutional neural network for mobile devices. In *Proceedings of the IEEE conference on computer vision and pattern recognition*, pages 6848–6856, 2018.
- [64] Ying Zhang, Tao Xiang, Timothy M Hospedales, and Huchuan Lu. Deep mutual learning. In *Proceedings of the IEEE conference on computer vision and pattern recognition*, pages 4320–4328, 2018.
- [65] Borui Zhao, Quan Cui, Renjie Song, Yiyu Qiu, and Jiajun Liang. Decoupled knowledge distillation. In *Proceedings of the IEEE/CVF Conference on computer vision and pattern recognition*, pages 11953–11962, 2022.
- [66] Helong Zhou, Liangchen Song, Jiajie Chen, Ye Zhou, Guoli Wang, Junsong Yuan, and Qian Zhang. Rethinking soft labels for knowledge distillation: A bias–variance tradeoff perspective. In *International Conference on Learning Representations*.